INTERNATIONAL JOURNAL OF TECHNO-ENGINEERING
IJTE

ISSN: 2057-5688

A REVIEW OF PIEZOELECTRIC MEMS SENSORS AND ACTUATORS FOR GAS DETECTION APPLICATION

Suneeta Seelam, Research Scholar, Department of Electronics and communication Engineering, Monad University, Hapur, U.P.

Dr.Jaidev Sharma, Associate Professor, Supervisor, Department of Electronics and communication Engineering, Monad University, Hapur, U.P.

Abstract

Piezoelectric microelectromechanical system (piezo-MEMS)-based mass sensors including the piezoelectric microcantilevers, surface acoustic waves (SAW), quartz crystal microbalance (QCM), piezoelectric micromachined ultrasonic transducer (PMUT), and flm bulk acoustic wave resonators (FBAR) are highlighted as suitable candidates for highly sensitive gas detection application. This paper presents the piezo-MEMS gas sensors' characteristics such as their miniaturized structure, the capability of integration with readout circuit, and abrication feasibility using multiuser technologies. The development of the piezoelectric MEMS gas sensors is investigated for the application of low-level concentration gas molecules detection. In this work, the various types of gas sensors based on piezoelectricity are investigated extensively including their operating principle, besides their material parameters as well as the critical design parameters, the device structures, and their sensing materials including the polymers, carbon, metal–organic framework, and graphene.

1 Introduction

Micro electromechanical systems (MEMS) originally referred to the integration of the mechanical and electrical components at the microscale and nanoscale dimensions. The main purpose and function of the MEMS are to collect physical and chemical information such as pressure, temperature, chemical and gases molecules from the surrounding environment and deliver this information in a more suitable form to human senses [1]. Undoubtedly, the task of gathering and transforming information is usually performed by

sophisticated technical systems. However, MEMS devices are capable to perform these tasks despite their small sizes [2]. In addition, MEMS can be defned as miniaturized mechanical and electromechanical elements that are made through microfabrication techniques with dimensions varying from below
one micron in the smallest elements all the way to several millimeters [2–7]. MEMS devices have been designed in several structural varying from simple structural with an element that does not perform any movement to extremely complex electromechanical system that contained multiple elements that performed sophisticated action and movement under the control of integrated microelectronic circuits [8].

The well-addressed components of the MEMS devices are the microsensors and microactuators, also known as "transducers," which are defned as the elements that perform the task of converting the energy or power from one domain to other domains [9]. For instance, the sensors can convert a measured physical signal into an electrical signal, whereas the actuators can convert the electrical signals into mechanical signals just to move themselves or any other components from one position into another state inside the system. In particular, the sensors are the devices that detect and monitor events or changes in the environment such as gas, chemical, pressure, temperature, vibration, and fow. On the other hand, the actuator transducer is the part of the system that helps to achieve physical/mechanical movement after receiving energy in the form of electrical or other forms of energy. There are various actuators such as pneumatic actuators [10] where their input is air, as well as piezoelectric actuators [11] where their inputs are current or voltage, the micro-valves for controlling the gas and liquid fows, as well as the micro-pumps for fuids pressures [12] that have been used in medical devices and many more. In fact, the output in the actuators is always in the mechanical form of energy [13]. In simple words, the sensing process can be defned as energy transduction that provides us with understanding signals or recognition of unknown actions, whereas the actuation process can be

ISSN: 2057-5688

classifed as the energy conversion that produces mechanical actions [14, 15].

In addition, MEMS is one of the most promising technologies of the twenty-frst century; it has the potential to signifcantly alter all aspects of our lives and the way we live in the future [16]. MEMS along with the combination of siliconbased micro electronics and micro machining technology has dramatically revolutionized both the industry technologies and consumer products from high-technology machines to tiny elements in smartphones. Scientists believe that the MEMS revolution is going to be the second revolution in micro manufacturing after the semiconductor micro fabrication revolution.

2 Litreature Survey

Sensing and actuation are only two of the many uses for ultrasound. In all of these industrial cleaning applications, therapeutic techniques including lithotripsy, tissue ablation, and ultrasound detection are essential. The coupling medium from the source must be used to detect the imparted ultrasonic. Wafer temperature is measured using a solid coupling medium; liquid is utilized for NDE and medical applications; and gas is used for air-coupled applications. When utilized in fluid-coupled applications, a piezoelectric transducer has an impedance mismatch. MUTs are often used in acoustic and high-dynamic-range air transducer applications.

Both ultrasonic microscopy and ultrasound flow metering in medical treatment have been extensively researched. Since theoretical study inhibits actual implementation, there are still a lot of unexplored application areas. The necessity for piezoelectric transducers has decreased as a result of the capacitive transducer's success in acoustic applications, impedance matching, wide bandwidth, and high-frequency applications. It is much less costly than a piezoelectric transducer since photolithography is used. An insulating layer sits on top of a conductive Si substrate to form the bottom electrode of a micro-dimensional capacitive element. An actuation layer made of metalized polysilicon that is conducting is printed onto the top electrode. An insulation layer on the conductive substrate prevents parallel

ISSN: 2057-5688

electrodes from touching one another and, by insulating the device, raises the collapse voltage. Acoustic sensors have been utilized for underwater imaging since the early 20th century. At the turn of the century, a critical mass had been achieved in the development of piezoelectric materials. Significant advancements in computer technology call for increasingly complex algorithms for transducer performance assessment. Through the use of micro fabrication technology, air gaps are decreased as a consequence of technical empowerment. In order to compete with piezoelectric sensors, capacitive electrostatic transducers may generate strong electric fields. Enhanced uses of CMUTs include integration with microelectronics, higher bandwidth, and huge arrays with connected electrical connections.

Rapid advancements in characterisation methods and a sound understanding of functioning principles have both significantly enhanced. The device's conception, manufacture, and methods are all improved by a fruitful behavioral approach research. Non-contact optical profilometers, which use optical interferometry to scan the surface of the CMUT in a microscopic environment, are significantly impacted by the CMUT's static behavior. The formulas demonstrate a relationship between the input and output variables as well as the structural requirements using finite element method (FEM) simulation. The benefits of CMUTs are many, and they include increased bandwidth, massive manufacturing techniques, superior sensitivity, and short reaction times.

Due to intensive research, CMUTs have lately been able to overcome the difficulties of fabricating two-dimensional arrays and are now able to capture real-time three-dimensional pictures. High power transmission requires a collapsed mode CMUT with correct biasing [18–19]. It is difficult to make an air-coupled ultrasonic transducer array that runs at 40 KHz and doesn't have grating lobes. When doing acoustic imaging in the presence of air, the size of the grating lobes presents a restriction. A one-dimensional air-coupled phased array transducer that can operate at 40 KHz is created by excluding the grating lobes. This obstacle may be avoided by keeping the transducer size under 4.3 mm.

Many researchers have created various manufacturing methods for CMUT. These techniques include wafer bonding, bulk micromachining, and surface micromachining. They may also be combined. At Stanford University, surface micromachining was used to manufacture CMUT for the first time. This procedure involves the formation of a bottom electrode on a non-conductive substrate, followed by the deposition of a sacrificial layer. By pre-patterning the sacrificial layer and afterwards constructing an anchor with the membrane around it, as illustrated, better dimensional control of the membrane is accomplished in this procedure. The membrane's structural layer is then placed on top of it, and release apertures are used to etch it. By removing the sacrificial layer, the membrane of the device is therefore hung onto the substrate.

3 Methodology

In recent years, ultrasonic transducers have been extensively employed in clinical imaging, using ceramics, piezoelectric materials, composites with various crystals, and piezo composite materials. The scientific community has developed MUTs as a remedy for the limitations of piezoelectric transducers. A particular form of MUT called a CMUT modulates electrostatic force by first altering capacitance. Fabrication may be done using a high-temperature fusion bonding method or a surface micromachining technology. In order to build the diaphragm of a conventional CMUT, which is supported on a fixed bottom electrode, square, circular, or hexagonal shape is included. The construction is similar to a capacitor in Fig. 3.1 because the bottom electrode is isolated from the top electrode by a tiny cavity filled with vacuum or air.

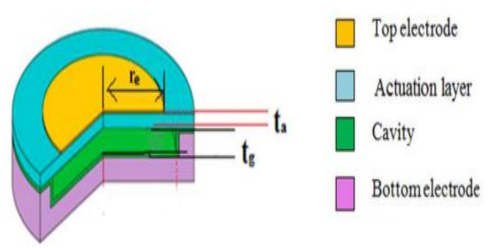

Fig. 3.1 3D view of circular non-insulated cell

A typical CMUT's dimensions include structural layer thickness of 750 nm with a 50 m diameter, cavity height of 1 m, and top electrode thickness of 50 nm, which are all often utilized for medical imaging. In order to assist the design of an electrostatic actuator for medical imaging for greater sensitivity, several

ISSN: 2057-5688

research publications have been examined taking this dimension into consideration. The top electrode functions as a diaphragm and is free to move or deform in relation to the bottom electrode in this capacitive action-based transducer's working principle. As a consequence, a change in the distance between these two electrodes causes a fluctuation in capacitance.

It may thus be regarded as a capacitor cell as it is made up of a thin, mobile film hung over a vacuum gap. One of the electrodes for the capacitor is sometimes the top electrode of the device, which occasionally develops a metal coating. Resonance occurs during transmitting mode as a result of applying bias voltage to the geometry and superimposing the desired signal on top of it. The result is the generation of an electrostatic force, which causes the diaphragm to vibrate and trigger an ultrasonic vibration in the medium around it. The device is exposed to the incident ultrasonic wave when in the receiving mode, and as a consequence, the sound pressure causes the diaphragm to deform in the direction of the fixed bottom electrode. Capacitance varies in direct proportion to the fluctuation in the distance between the top and bottom electrodes. A appropriate microelectronic circuit then converts the change in capacitance to an equivalent electrical signal. This capacitive element is increasingly being regarded as a MEMS with a capacitive operating principle due to the accumulation of mechanical components and microelectronic circuits.

The hexagonal CMUT structure outperforms the rectangular, circular, and square ones in terms of packing density. For hexagonal layers, a circular approximation is often used for mathematical simplicity. The structural layer will deform, causing a sharp change in the capacitance between the deformed layer and the fixed electrode.

This shape function is accurately taken into account during analytical modeling of deflection to explain the deflection of the deformed layer. Additionally, the impact of certain geometry factors is examined using this shape function. Numerous writers have conducted extensive research on the deflection form functions of square and circular geometries. Since rectangular layers perform better than square ones and have shown potential to increase fill factor, modeling of rectangular layers is also worthwhile to investigate. Based on various test experiments, the circular geometry exhibits good repeatability, can be used for long-range underwater object detection, distance measurement, and high intensity frequency applications. It also exhibits the highest deflection among geometrical structures. Metals like nickel and aluminum, nonmetals like silicon (Si) and germanium (Ge), polymers like SU8 and polyamide like diamond, silicon carbide (SiC), silicon nitride (Si3N4), and silicon dioxide (SiO2) are among the materials utilized for structural layers [10–12]. One of the best materials to employ that is excellent at both producing and detecting ultrasonic waves in the air is Si3N4. High pressure transmission may increase penetration and improve signal to noise ratio. In addition to all of these properties, CMUT may be used in imaging applications where tissue heating is common. SiC is the material that is most suitable for this kind of application. When compared to Si3N4, SiC will allow for manufacturing at lower temperatures, and it can be used to create high frequency applications since it has superior mechanical and electrical characteristics. Typically, SiO2 is utilized to create the dielectric spacer while the transmitter is in full swing in transmit mode or while the receiver is in folded operation, the gap between the top and bottom electrodes may be crossed during operation and may result in an electrical shock. Due to capacitive action, a strong electric field is created between the two electrodes that are charged in opposition to one another, creating an electrical danger and adhesion force. When employed in biomedical imaging, the risks brought on by inadequate insulation are of concern [13]. Analytical modeling and characterization research on a SiC-based insulated CMUT are used to demonstrate the need of an insulation layer.

In order to guard against electric shock, there is a high-K dielectric layer between the electrodes. The top electrode may be patterned at the bottom surface of the actuation layer thanks to the inclusion of an insulating layer, as illustrated in Fig. 3.2 (a). Figure 3.2(b) illustrates a construction without an insulating layer, with the actuation layer positioned immediately under the top

ISSN: 2057-5688

electrode to protect against electric shock.

The two electrical layers' different work functions increase the electrostatic force between the substrate and the surface, which is sufficient to cause electrons to move between them. The energy drops off as the top electrode makes contact with the bottom one, and it stayed stuck until the total removal energy dropped to its lowest point. The surface feels this total energy, which consists of energy that has been restored for deformation and attraction. The insulating layer's dielectric material is chosen in such a way that it can withstand the electric field produced within the apparatus as a result of electrostatic attraction force.

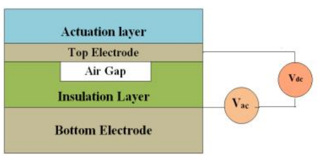

Fig. 3.2 (a) Insulated Structure

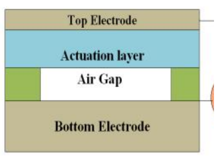

Fig 3.2 (b) Non-insulated Structur

[14-16]. The selection of high-K dielectric material should improve the efficiency for generating high electric field by not reducing the transduction gap and without further increasing in bias voltage both in transmitting and receiving mode, as designing of sensitive CMUT is the most crucial criterion. The majority of high-K materials with a dielectric constant (K) range between 3.9 and 200 are well described in literature [17]. This suggests that when the value of the dielectric constant rises, the breakdown strength Ebd of a dielectric substance falls. According to the description provided by thermochemical characteristics, K-1/2 seems to reduce final breakdown strength. Due to their inadequate breakdown strength, which is crucial for maintaining isolation thickness in the nanoscale range, all high-K materials are therefore not at all a viable solution. Hafnium dioxide (HfO2) may be taken into account after taking all of these phenomena into account since it maintains a balance between its disintegration strength and dielectric constant, which is required for low temperature production processes in nano dimensional features.

4. **Result Evaluation**

The electric field bends at the borders and extends to nearby remote areas as the fringing fields in a CMUT structure because the thickness of the actuation layer and gap spacing equals the diameters of the electrodes. The device's equivalent capacitance is increased by the fringing field. The charge-storing effect, however, is also a result of the fringing field, which also affects the linked capacitance. Younes Ataiiyan's technique [18] could be practical to establish their connection in a circular-disk capacitor. It accepts the static deformation supported by the fringing field and polarizing voltage. As a consequence, a displacement profile with fringing effect supports the results of the simulations and experiments more strongly than one without it. The fringing field with appropriate boundary settings must be taken into account in order to simulate the capacitance.

The actuation layer, the cavity, and the insulating layer all exhibit fringe capacitances. Both the capacitance and the electrostatic force grow. [22–24] discusses the effects of a fringing field in an electrostatic actuator and a time-varying serial capacitor of various types. The control of parallel-plate electrostatic microactuators is practical with this capacitor [25]. Additionally, the present strategy is based on useful rules that were drawn from studies of ultrasonic waves. These capacitance prototypes have also been used in some more recent research, where an updated capacitance model for radiofrequency (RF) MEMS shunt switching that integrates the effects of the perforated beam's fringing field is developed [26]. Additionally, the square diaphragm CMUT for the fringing field effect has been studied. A non-insulated element, as shown in Fig. 3.2(b), consists of a deeply doped Si layer that is covered by a thin metalized actuation layer with a thickness of 750 nm and an electrode diameter of 50 m. The bottom electrode is created by metalizing the Si base's top surface [9]. Si3N4 and SiC are compared as actuation layers in this investigation. The CMUT is supported by SiO2 pillars. Aluminum (Al) is produced as the top metal for the metallization. The direct capacitances for the gap and actuation layers of a completely metalized CMUT are,

$$C_g = \left\{ \left(\varepsilon_g A \right) / t_g \right\}$$

$$C_a = \left\{ \left(\varepsilon_a A \right) / t_a \right\}$$

Where 2 A r e stands for the area of the electrodes and e r is the radius of the electrode, and where g t is gap separation and a t is the thickness of the actuation layer. K a g a stands for the permittivity of the actuation layer and has a value of 8.85 10-12 C 2 /(N-m2).

ISSN: 2057-5688

K an is the relative dielectric constant. The formula for equivalent device capacitance is

$$C_{eq} = \left(C_a \times C_g\right) / \left(C_a + C_g\right)$$

$$\frac{1}{C_{eq}} = \frac{t_g}{\varepsilon_g A} + \frac{t_a}{K_a \varepsilon_g A} = \frac{\varepsilon_g A}{t_g + \frac{t_a}{K_a}}:$$

A compact technique is available as Landau and Lifschitz approach. In this method the effective capacitance including fringing is,

$$C = \frac{\varepsilon \pi r^2}{d} + \varepsilon r \ln\left(\frac{16\pi r}{d} - 1\right)$$

ε is the permittivity of the dielectric, r and d are the radius and the separation between the electrodes respectively. Considering fringing effect, the total capacitance of the gap is Cgf and that of actuation layer is Caf . This gives, the following (3.6) and (3.7) respectively,

$$C_{gf} = \varepsilon_g \left[\left(\frac{\pi r_e^2}{t_g}\right) + r_e \ln\left\{\left(\frac{16\pi r_e}{t_g}\right)\right.\right.$$

$$C_{af} = \varepsilon_a \left[\left(\frac{\pi r_e^2}{t_a}\right) + r_e \ln\left\{\left(\frac{16\pi r_e}{t_a}\right) - \right.\right.$$

Now the equivalent capacitance due to fringing Ceqf can be denoted as the series capacitance of the actuation layer and the air gap capacitance. Therefore it is written as,

$$C_{eqf} = \left(C_{af} \times C_{gf}\right) / \left(C_{af} + C_{gf}\right)$$

Putting the expressions of (3.6) and (3.7), in (3.8), it can be expressed as

$$C_{eqf} = \frac{\left\{\frac{\varepsilon_g \pi r_e^2}{t_g} + \varepsilon_g r_e \ln\left(\frac{16\pi r_e}{t_g} - 1\right)\right\}\left\{\frac{K_a \varepsilon_g \pi r_e^2}{t_a} + K_a \varepsilon_g r_e \ln\left(\frac{16\pi r_e}{t_a} - 1\right)\right\}}{\left\{\frac{\varepsilon_g \pi r_e^2}{t_g} + \varepsilon_g r_e \ln\left(\frac{16\pi r_e}{t_g} - 1\right)\right\} + \left\{\frac{K_a \varepsilon_g \pi r_e^2}{t_a} + K_a \varepsilon_g r_e \ln\left(\frac{16\pi r_e}{t_a} - 1\right)\right\}}$$

$$C_{eqf} = \frac{\left\{\frac{\pi r_e}{t_g} + \ln\left(\frac{16\pi r_e}{t_g} - 1\right)\right\}\left\{\frac{K_a \pi r_e}{t_a} + K_a \ln\left(\frac{16\pi r_e}{t_a} - 1\right)\right\}}{\left\{\frac{\pi r_e}{t_g} + \ln\left(\frac{16\pi r_e}{t_g} - 1\right)\right\} + \left\{\frac{K_a \pi r_e}{t_a} + K_a \ln\left(\frac{16\pi r_e}{t_a} - 1\right)\right\}} \quad (3.9)$$

Analyzing the transducer performance with different settings requires both analytical modeling and simulation techniques, which are equally important. This computing method only relies on mathematical generalization to provide a straightforward analysis for examining the properties. As it primarily deals with the linear connection between actuation layer deflection and applied force, it is limited in its ability to represent a real-time device. By using simulation approach and analytical modeling, accuracy and precision may be improved.

ISSN: 2057-5688

5 Conclusion

This chapter discusses the Landau method for modeling the CMUT fringing field implication. The actuation layer, gap, and insulation capacitances are calculated using this method. SiC is a structural material that makes the CMUT more capable of being made with the shortest thermal budget because to its high Young modulus and low residual stress. The CMUT can work securely in high-voltage applications and remain stable at high temperatures because to the inclusion of an insulating layer, which also increases device selectivity. The insulating layer is very helpful in enabling CMUT to provide high-resolution imaging at an affordable price, which may aid in the development of medical imaging.

The simulation's outcome supports Landau and Lifschitz's methodology for simulating the fringing field effect in CMUT. The simulation's output comes the closest to accurately representing how different variables affect a device's capacitance. Using the atomic layer deposition (ALD) method, it is also feasible to employ HfO2 in low-temperature production with an isolation thickness of under 100 nm. When HfO2 is employed as an insulating layer in place of Si3N4, the performance of CMUT is enhanced in every way. The CMUT's properties have been improved, making it more sensitive for high-frequency applications and suitable for usage in acoustic media. A CMUT's performance in a high-intensity application depends on its displacement, frequency, and impedance profile.

6. References

[1] Seyed M Allameh 2006 Advanced Structural Materials: Properties, Design Optimization, and Applications.

[2] P Muralt 2000 Ferroelectric thin films for micro-sensors and actuators J. Micromech. Microeng. 136–146.

[3] N Setter, D Damjanovic, L Eng, G Fox, S Gevorgian, S Hong et.al 2006 Ferroelectric thin films: Review of materials, properties and applications Journal of Applied Physics 100.

[4] Wasa K, Kanno I, Kotera H, Yamauchi N, Matsushima T 2008 Thin films of PZT-based ternary perovskite compounds for MEMS Proc. of IEEE International Ultrasonics Symp, 213-216.

ISSN: 2057-5688

[5] Zhang Z, Li X and Chen 2000 J, Journal of Tianjin University 33 378-381.

[6] Naoki W, Kazumasa K and Yi X 2000 Thin Solid Films 372 156-162.

[7] L HENCH and J WEST 1990 The Sol-Gel Process, Chem.Rev. 90 33-72.

[8] I Y (Steve) Shen, G Z Cao, Chia-Che Wuand Cheng-Chun Lee 2006 PZT Thin-Film Meso- and Micro Devices Ferroelectrics 342 15–34.

[9] Klein L 1994 Sol-Gel Optics: Processing and Applications Springer Verlag. ISBN 0792394240.

[10] Hirano S I, Yogo T and Tikuta K 1992 J Am. Ceram. Soc.75 2785-90.

[11] S K Pandeya, A R Jamesa, R Ramana, S N Chatterjeea et.al 2005 Structural, ferroelectric and optical properties of PZT thin films Physica B, science direct 369 135–142.